Supporting Information

Nitrogen Vacancies Modulated Efficient Ammonia Desorption over metal-free BC_3N_2 monalayer

Long Lin[a] , Kun Xie[a], Chaozheng He[b,c]*,

[a] *Henan Key Laboratory of Materials on Deep-Earth Engineering, School of Materials Science and Engineering, Henan Polytechnic University, Jiaozuo, 454000, Henan, China*

[b] *Institute of Environmental and Energy Catalysis, School of Materials Science and Chemical Engineering, Xi'an Technological University, Xi'an 710021, China*

[c] *Shaanxi Key Laboratory of Optoelectronic Functional Materials and Devices, School of Materials Science and Chemical Engineering, Xi'an Technological University, Xi'an 710021, China*

*Author to whom correspondence should be addressed.

E-mail address: hecz2019@xatu.edu.cn (C. He);

Number of Pages: 9

Number of Notes:1

Number of Figures:9

Number of Tables: 9

Note S1. Gibbs free energy calculation

Free energies of the NRR intermediates in electrochemical reaction pathways were calculated based on the computational hydrogen electrode (CHE) model proposed by Nørskov et al. [1] The chemical potential of the H^+/e^- pair was considered as half of the gas-phase H_2. Thus, the change of Gibbs free energy (ΔG) for each reaction step was given by：□ □ □ □ □ □ □

$$\Delta G = \Delta E + \Delta ZPE - T\Delta S + \Delta G_U + \Delta G_{pH} \qquad \text{(S-1)}$$

where ΔE is calculated directly by DFT, ΔZPE is the zero-point energy correction, T is the temperature (T = 298.15 K), and ΔS is the change in entropy. ΔG_U is the contribution of the electrode potential (U) to ΔG, and $\Delta G_{pH} = k_B T \times \ln 10 \times pH$, where k_B is the Boltzmann constant under standard reaction conditions.

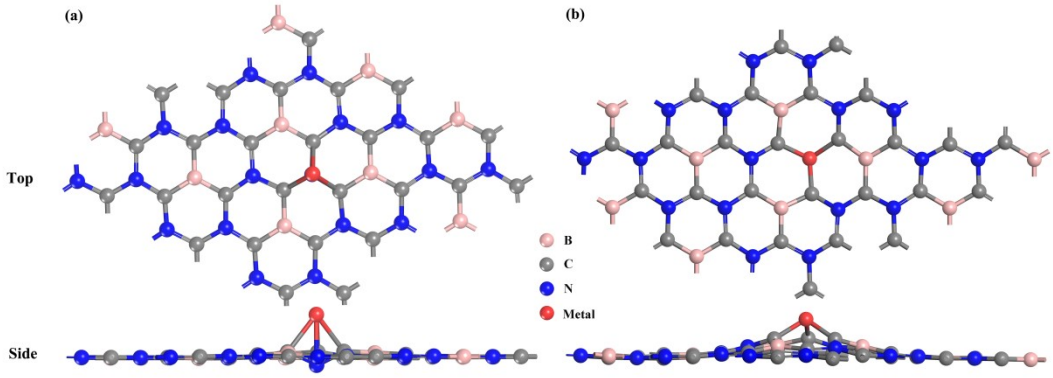

Fig. S1 The top and side views for the relaxed structures of TM@ BC_3N_2 model (a) and V_N-TM@BC_3N_2 model (b). Colored spheres are B (pink), C (gray), N (blue) atom and Metal (jacinth).

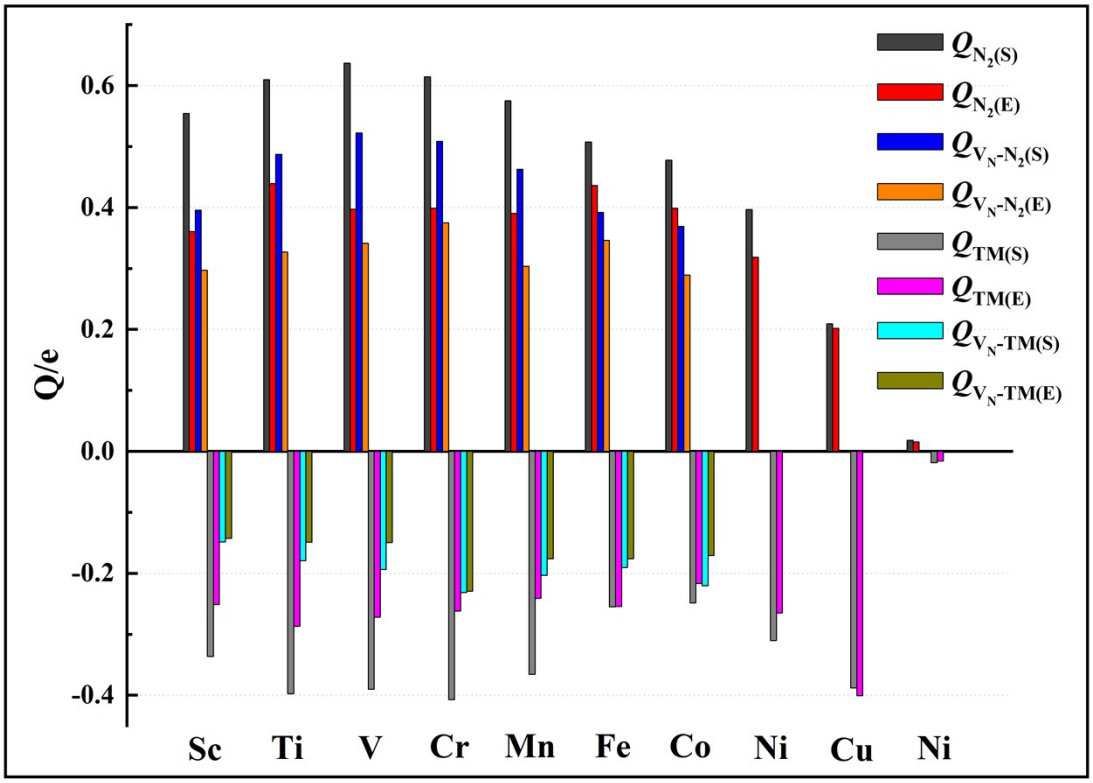

Fig. S2 Relationship between calculated charge transfer from the catalyst to N_2 ($\triangle Q_{N_2(S/E)}$, $\triangle Q_{V_N\text{-}N_2(S/E)}$) and charge transfer of TM before and after N_2 adsorption ($\triangle Q_{TM(S/E)}$, $\triangle Q_{V_N\text{-}TM(S/E)}$).

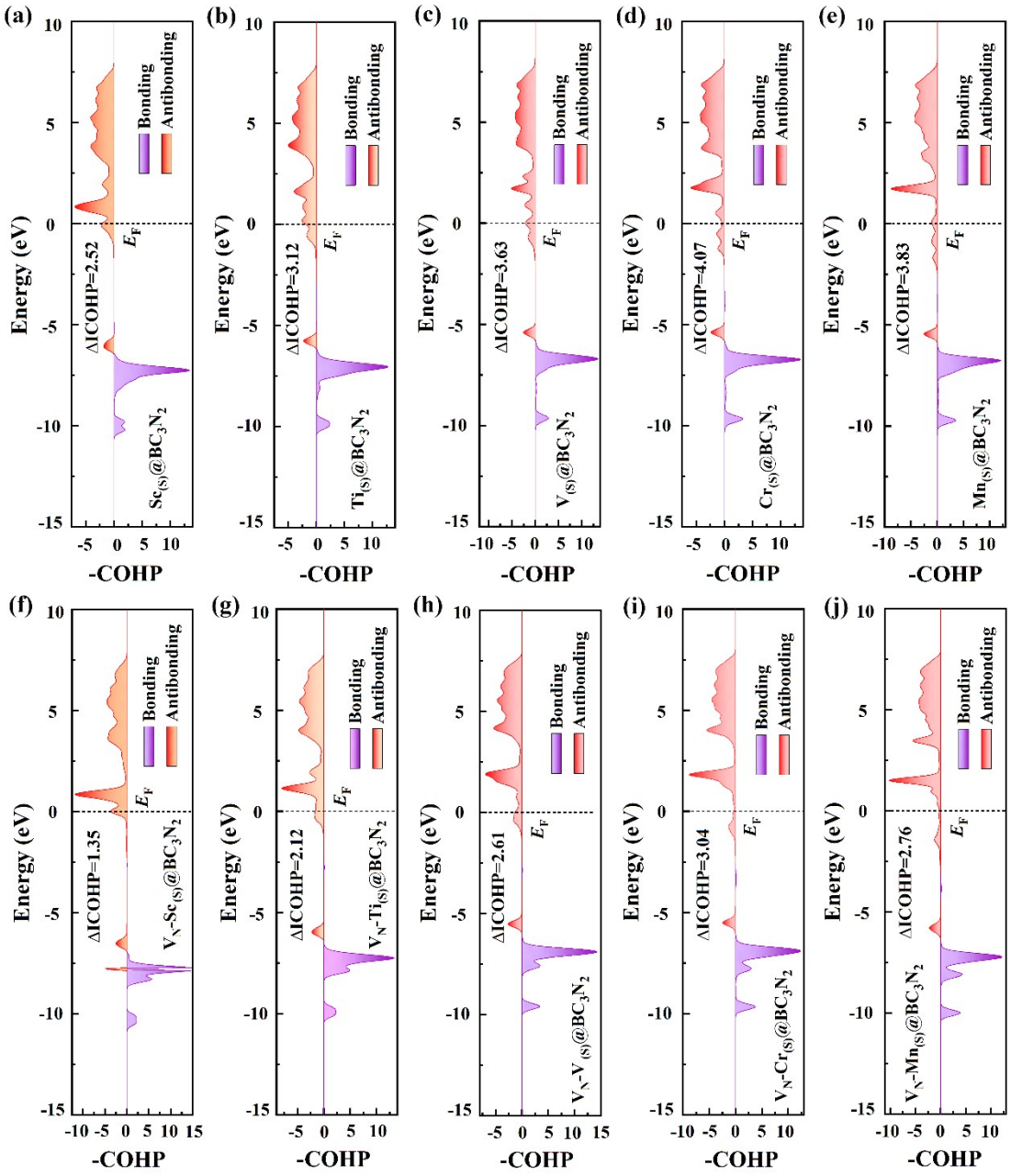

Fig. S3 Crystal Orbital Hamilton Population (COHP) between the two single atoms of nitrogen when N_2 horizontal adsorption on TM@BC_3N_2 and V_N-TM@BC_3N_2 (TM=Sc, Ti, V, Cr, Mn).

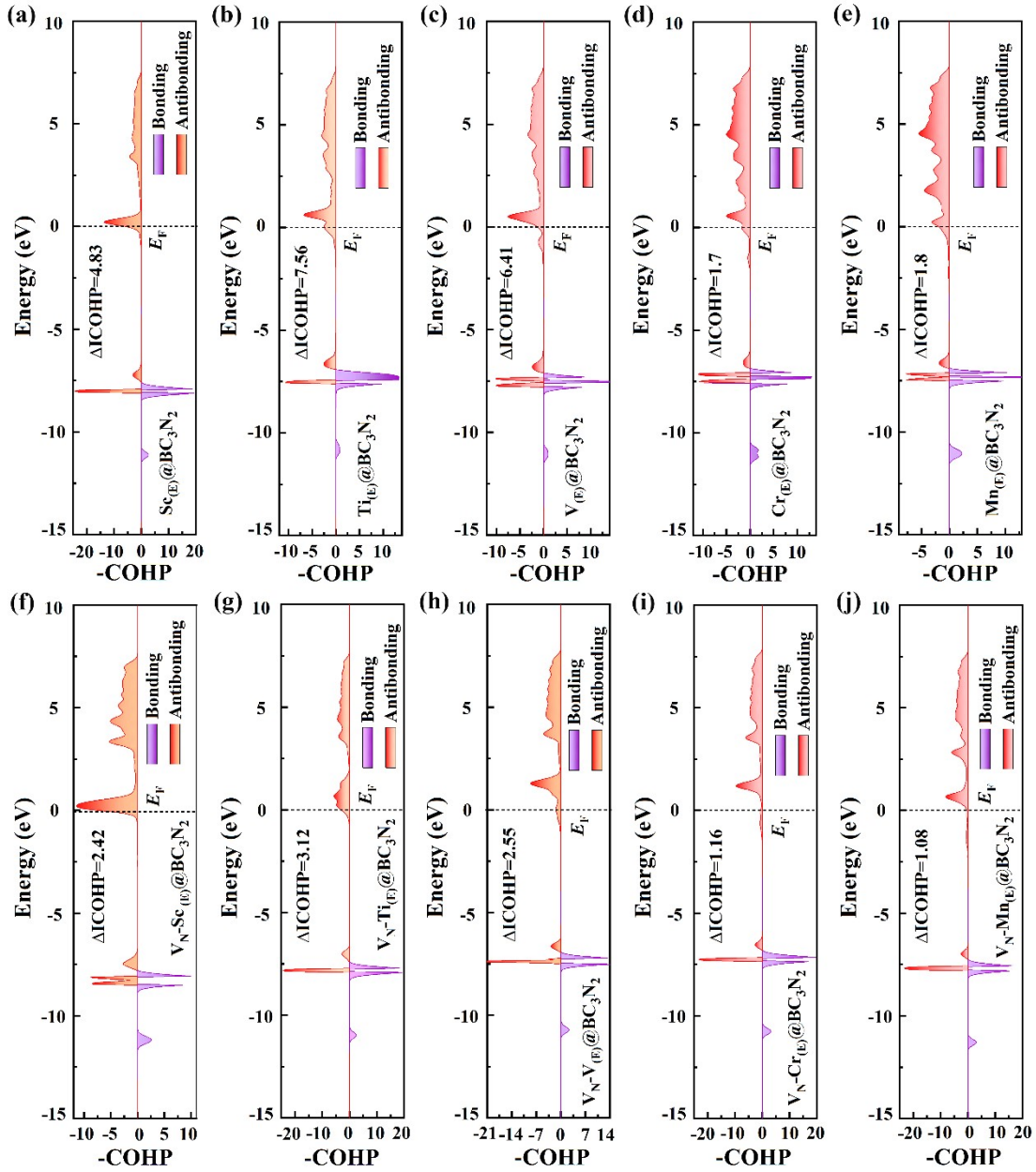

Fig. S4 Crystal Orbital Hamilton Population (COHP) between the two single atoms of nitrogen when N_2 vertical adsorption on $TM@BC_3N_2$ and V_N-$TM@BC_3N_2$ (TM=Sc, Ti, V, Cr, Mn).

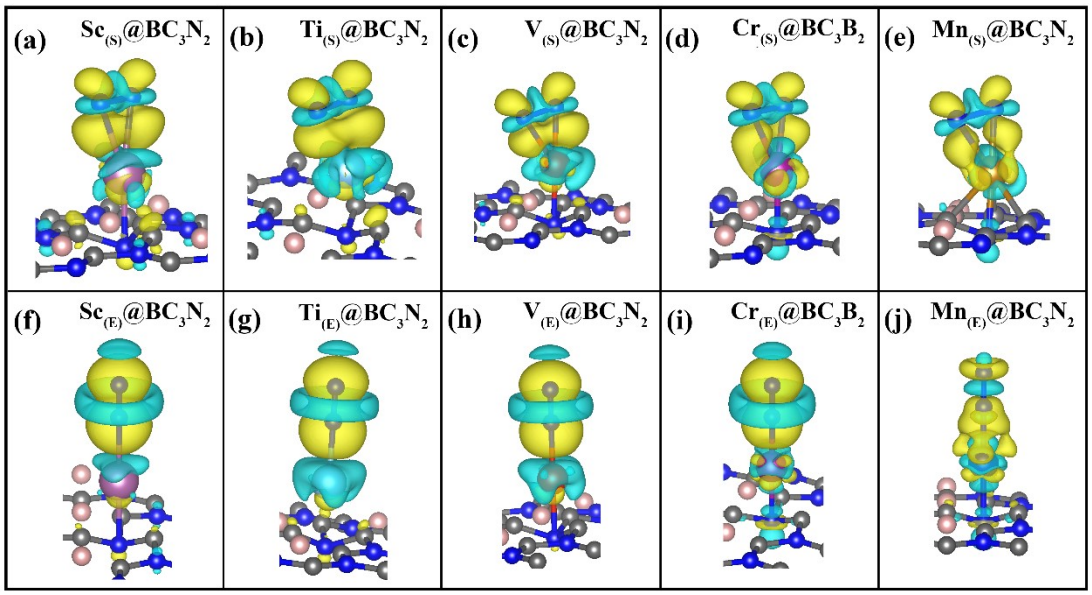

Fig. S5 The difference charge of N_2 horizontal and vertical adsorpted on $TM@BC_3N_2$ (TM=Sc, Ti, V, Cr, Mn). The isosurface value is 0.003 e/Å. The bule region represents the electron accumulation, while yellow blue region corresponds the electron loss.

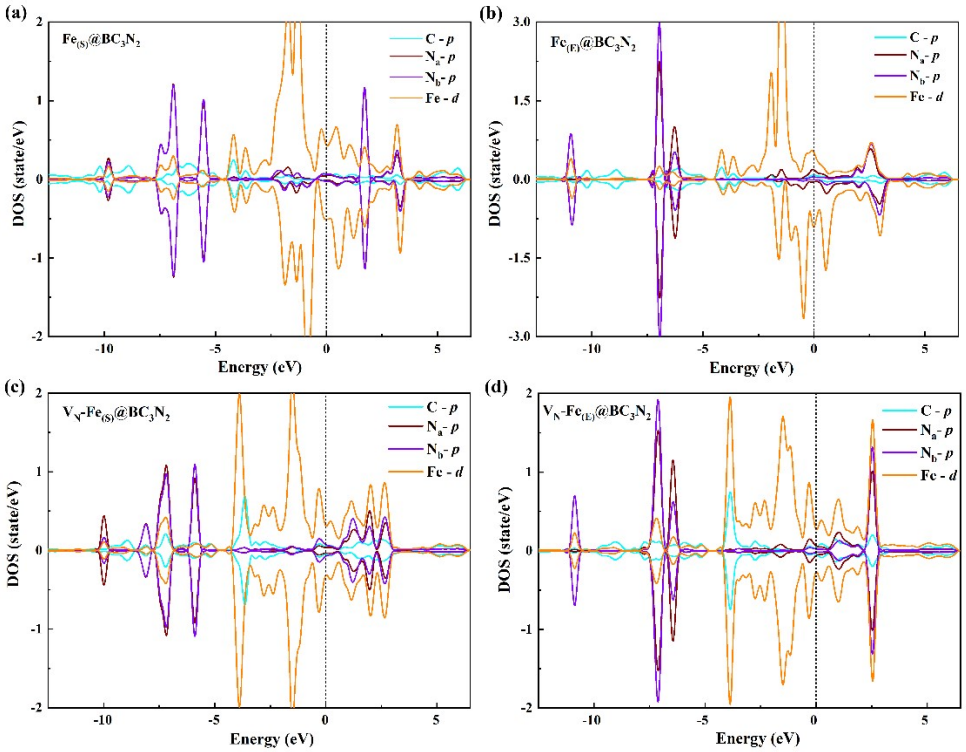

Fig. S6 (a)-(d) The density of states (DOS) plots of N_2 end-on and side-on adsorption on $Fe/V_N\text{-}Fe@BC_3N_2$ system.

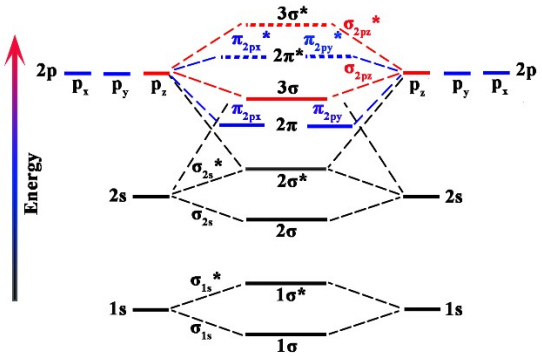

Fig. S7 Molecular orbital diagram of nitrogen.

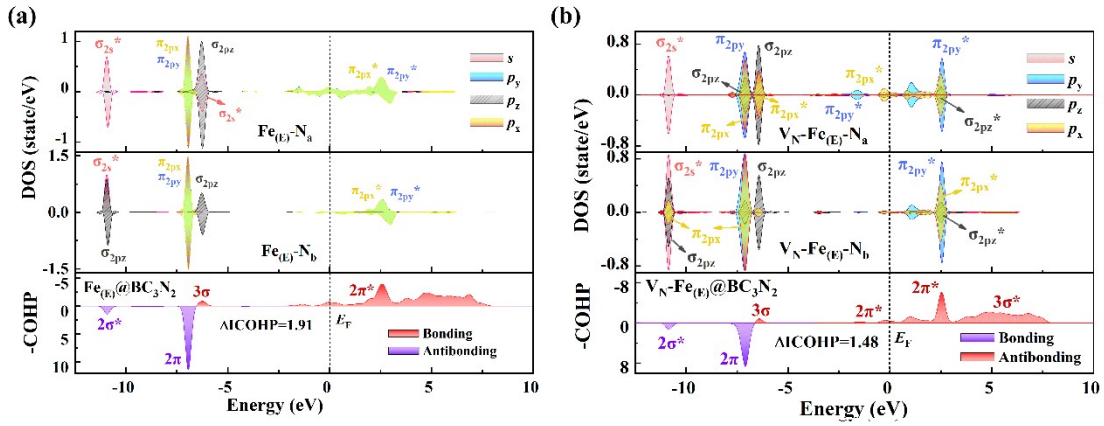

Fig. S8. (a) and (b) are the PDOS of two single atoms of nitrogen and the Crystal orbital Hamilton population (COHP) between N-N of adsorbed N_2 when N_2 end-on adsorption on Fe/V_N-Fe@BC_3N_2.

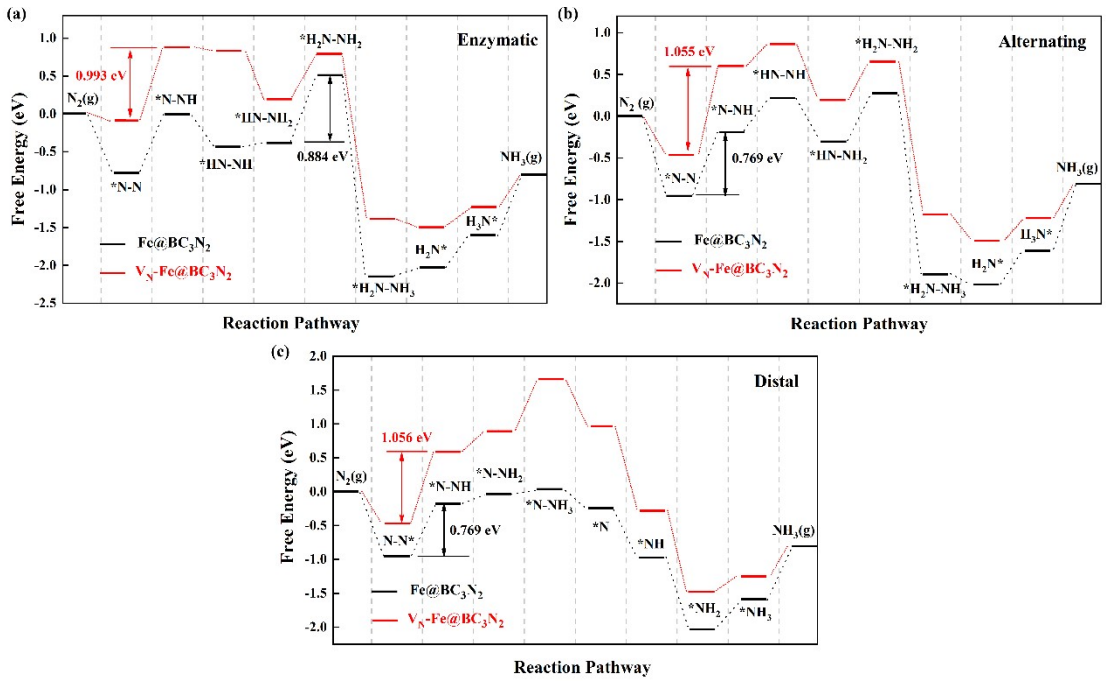

Fig. S9. Free energy diagrams for N_2 reduction on Fe/V_N-Fe@BC_3N_2 through (a) enzymatic, (b) alternating, and (c) distal mechanisms.

Table S1 Summary of lattice constant a, b, bond length d_1, d_2, and bond angle α, β, γ (see Fig. 1(a)) for BC_3N_2.

	a (Å)	d_1 (Å)	d_2 (Å)	α (°)	β (°)	γ (°)
BC_3N_2	4.277	1.395	1.482	120.0	117.9	124.2

Table S2 The calculated results for Sc to Zn adsorbed on BC_3N_2 monolayer. The adsorption energy, Bader charge and bond length between TM and the closest B, C, N atoms.

Configurations	E_b (eV)	Bader charge	Bond length (Å)		
Metal-site		(e)	Metal-B	Metal-C	Metal-N
Sc-T_B	-2.10	-0.961	2.320	2.354	3.159
Sc-H	-2.65	-1.319	2.567	2.140	2.330
Sc-T_N	**-3.29**	**-1.179**	**3.062**	**2.203**	**2.240**
Ti-T_B	-2.32	-0.811	2.233	2.294	3.11
Ti-H	-2.80	-0.866	2.364	2.09	2.45
Ti-T_N	**-3.47**	**-1.056**	**2.97**	**2.104**	**2.149**
V-T_B	-1.96	-0.65	2.167	2.262	3.089
V-H	-2.12	-0.732	2.303	2.099	2.516
V-T_N	**-2.65**	**-0.891**	**2.975**	**2.063**	**2.067**
Cr-T_B	-0.74	-0.357	2.235	2.539	3.259
Cr-$B_{B\text{-}C}$	-0.90	-0.393	2.46	2.107	2.964
Cr-H	-0.88	-0.397	2.283	2.106	2.787
Cr-T_N	**-1.36**	**-0.711**	**2.969**	**2.076**	**2.198**
Mn-T_B	-0.74	-0.443	2.224	2.449	3.206
Mn-$B_{B\text{-}C}$	-0.75	-0.43	2.279	2.189	3.053
Mn-T_N	**-1.28**	**-0.619**	**3.01**	**2.146**	**2.202**
Fe-T_B	-1.36	-0.296	2.048	2.168	2.957
Fe-T_C	-1.38	-0.21	2.316	1.955	2.822
Fe-H	-1.68	-0.4	2.166	2.027	2.447
Fe-T_N	**-1.89**	**-0.48**	**2.94**	**2.073**	**2.124**
Co-T_B	-2.18	-0.318	1.92	2.066	2.93
Co-$B_{B\text{-}C}$	-1.95	-0.052	2.152	1.893	2.806
Co-H	-2.37	-0.29	2.07	1.952	2.415
Co-T_N	**-2.55**	**-0.35**	**2.861**	**1.94**	**2.177**
Ni-T_B	-2.23	-0.141	1.935	2.236	2.035
Ni-$B_{B\text{-}C}$	-2.62	0.025	2.092	1.862	2.783
Ni-H	**-2.65**	**-0.167**	**2.253**	**1.954**	**2.371**

Ni-T_N	-2.52	-0.285	2.0894	2.021	2.207
Cu-T_B	-1.27	0.148	2.074	2.815	3.481
Cu-T_C	**-1.37**	**-0.065**	**2.720**	**1.965**	**2.773**
Cu-T_N	-0.78	-0.187	3.044	2.248	2.328
Zn-T_B	-0.16	-0.015	3.033	3.372	3.393
Zn-B_{B-C}	-0.16	-0.021	3.122	3.146	3.578
Zn-B_{C-N}	-0.15	-0.026	3.549	3.111	3.147
Zn-T_C	-0.15	-0.025	3.348	3.055	3.379
Zn-H	**-0.17**	**-0.027**	**3.261**	**3.273**	**3.030**
Zn-T_N	-0.14	-0.025	3.905	3.356	3.095

Table S3 The anchor atoms adsorption energy (E_b), the charge transfer ($\triangle Q_{TM}$) of TM atom anchored to the BC_3N_2 nanosheet, the migration barrier of the TM on the substrate surface (E_{bar}), the nitrogen vacancy formation energy (E_{Vn}) directly below the TM anchoring site.

TM site	E_b (eV)	$\triangle Q_{TM}$	E_{bar} (eV)	E_{VN} (eV)
Sc-T_N	-3.29	-1.179	1.15	1.24
Ti-T_N	-3.47	-1.056	0.75	0.26
V-T_N	-2.65	-0.891	0.61	0.06
Cr-T_N	-1.36	-0.711	0.53	0.29
Mn-T_N	-1.28	-0.619	0.47	0.12
Fe-T_N	-1.89	-0.48	0.29	-0.37
Co-T_N	-2.55	-0.35	0.48	-0.05
Ni-H	-2.65	-0.167	0.09	/
Cu-T_C	-1.37	-0.065	0.31	/
Zn-H	-0.18	-0.027	0.01	/

Table S4 The N_2 adsorption energy ($E_{ad(E)/(S)}$) of TM atom anchored to the BC_3N_2 nanosheet.

TM site	N_2 site	$E_{ad(E)}$	$E_{ad\text{-}VN(E)}$	N_2 site	$E_{ad(S)}$	$E_{ad\text{-}VN(S)}$
Sc-T_N	**E**	-0.75	-0.54	**S**	-0.61	-0.37

Ti-T_N	-1.20	-0.87	-1.14	-0.69
V-T_N	-1.35	-1.16	-1.23	-0.90
Cr-T_N	-1.06	-1.31	-0.90	-0.97
Mn-T_N	-0.96	-1.11	-0.78	-0.80
Fe-T_N	-1.46	-0.97	-1.29	-0.58
Co-T_N	-1.47	-0.79	-1.10	-0.81
Ni-H	-1.38	-	-0.86	-
Cu-T_C	-0.77	-	-0.77	-
Zn-H	-0.03	-	-0.02	-

Table S5 The TM atoms' charge transfer ($\triangle Q_{TM}$) of TM atom anchored to the BC_3N_2 nanosheet, TM charge transfer ($\triangle Q_{TM(S)}$, $\triangle Q_{TM(E)}$) during nitrogen horizontal and vertical adsorption, TM charge transfer ($\triangle Q_{V_N\text{-}TM}$) in the presence of intrinsic nitrogen defects, the charge transfer of TM ($\triangle Q_{V_N\text{-}TM(S)}$, $\triangle Q_{V_N\text{-}TM(E)}$) after nitrogen horizontal adsorption and vertical adsorption in the presence of intrinsic nitrogen defects.

TM site	$\triangle Q_{TM}$	$\triangle Q_{TM(S)}$	$\triangle Q_{TM(E)}$	$\triangle Q_{VN\text{-}TM}$	$\triangle Q_{VN\text{-}TM(S)}$	$\triangle Q_{VN\text{-}TM(E)}$
Sc-T_N	-1.179	-1.516	-1.43	-1.491	-1.64	-1.634
Ti-T_N	-1.056	-1.456	-1.343	-1.447	-1.626	-1.595
V-T_N	-0.891	-1.281	-1.163	-1.2831	-1.477	-1.432
Cr-T_N	-0.711	-1.118	-0.973	-1.014	-1.246	-1.243
Mn-T_N	-0.619	-0.985	-0.86	-0.822	-1.025	-0.999
Fe-T_N	-0.48	-0.735	-0.734	-0.616	-0.807	-0.792
Co-T_N	-0.35	-0.599	-0.567	-0.497	-0.718	-0.668
Ni-H	-0.167	-0.478	-0.432	-	-	-
Cu-T_C	-0.065	-0.453	-0.466	-	-	-
Zn-H	-0.027	-0.045	-0.043	-	-	-

Table S6 The N_2 charge transfer ($\triangle Q_{N_2(S)}$, $\triangle Q_{N_2(E)}$) during nitrogen horizontal and vertical adsorption, the charge transfer of N_2 ($\triangle Q_{V_N\text{-}N_2(S)}$, $\triangle Q_{V_N\text{-}N_2(E)}$) after nitrogen horizontal adsorption and vertical adsorption in the presence of intrinsic nitrogen defects.

TM-site	$\triangle Q_{N2(S)}$	$\triangle Q_{N2(E)}$	$\triangle Q_{VN-N2(S)}$	$\triangle Q_{VN-N2(E)}$
Sc-T_N	0.554	0.361	0.396	0.297
Ti-T_N	0.609	0.439	0.487	0.327
V-T_N	0.637	0.397	0.522	0.341
Cr-T_N	0.614	0.399	0.508	0.375
Mn-T_N	0.575	0.390	0.463	0.303
Fe-T_N	0.508	0.436	0.392	0.346
Co-T_N	0.478	0.399	0.369	0.289
Ni-H	0.396	0.318	-	-
Cu-T_C	0.209	0.202	-	-
Zn-H	0.018	0.015	-	-

Table S7 The variation of N−N bond lengths in each configureations.

configurations	$\triangle d_{N-N}$	configureations	$\triangle d_{N-N}$	configureations	$\triangle d_{N-N}$	configureations	$\triangle d_{N-N}$
$Sc_{(S)}$	4.95%	$Sc_{(E)}$	2.33%	V_N-$Sc_{(S)}$	3.26%	V_N-$Sc_{(E)}$	1.78%
$Ti_{(S)}$	5.93%	$Ti_{(E)}$	2.97%	V_N-$Ti_{(S)}$	4.48%	V_N-$Ti_{(E)}$	2.04%
$V_{(S)}$	6.91%	$V_{(E)}$	2.67%	V_N-$V_{(S)}$	5.13%	V_N-$V_{(E)}$	2.21%
$Cr_{(S)}$	7.14%	$Cr_{(E)}$	2.84%	V_N-$Cr_{(S)}$	5.50%	V_N-$Cr_{(E)}$	2.26%
$Mn_{(S)}$	6.91%	$Mn_{(E)}$	2.86%	V_N-$Mn_{(S)}$	5.36%	V_N-$Mn_{(E)}$	2.15%
$Fe_{(S)}$	6.79%	$Fe_{(E)}$	2.78%	V_N-$Fe_{(S)}$	4.26%	V_N-$Fe_{(E)}$	2.40%
$Co_{(S)}$	6.27%	$Co_{(E)}$	2.60%	V_N-$Co_{(S)}$	3.30%	V_N-$Co_{(E)}$	2.06%
$Ni_{(S)}$	4.87%	$Ni_{(E)}$	2.14%				
$Cu_{(S)}$	1.52%	$Cu_{(E)}$	1.58%				
$Zn_{(S)}$	0.06%	$Zn_{(E)}$	0.06%				

Table S8 The computed ICOHPs for all N_2 adsorption configurations and the ICOHPs ($\triangle_{ICOHP}$) difference between N_2 adsorption configurations and isolated N_2 molecule.

Configurations	ICOHP	△ICOHP	Configurations	ICOHP	△ICOHP
$Sc_{(E)}$	-18.08	4.83	$Sc_{(S)}$	-20.4	2.52
$Ti_{(E)}$	-15.35	7.56	$Ti_{(S)}$	-19.79	3.12
$V_{(E)}$	-16.51	6.41	$V_{(S)}$	-19.28	3.63
$Cr_{(E)}$	-21.22	1.7	$Cr_{(S)}$	-18.85	4.07
$Mn_{(E)}$	-21.11	1.8	$Mn_{(S)}$	-19.08	3.83
$Fe_{(E)}$	-21.01	1.91	$Fe_{(S)}$	-19.21	3.71
$Co_{(E)}$	-21.13	1.78	$Co_{(S)}$	-	-
Configurations	ICOHP	△ICOHP	Configurations	ICOHP	△ICOHP
V_N-$Sc_{(E)}$	-20.50	2.42	V_N-$Sc_{(S)}$	-21.57	1.35

V_{N}-Ti $_{(E)}$	-19.80	3.12	V_{N}-Ti $_{(S)}$	-20.80	2.12
V_{N}-V $_{(E)}$	-20.37	2.55	V_{N}-V $_{(S)}$	-20.30	2.61
V_{N}-Cr $_{(E)}$	-21.76	1.16	V_{N}-Cr $_{(S)}$	-19.88	3.04
V_{N}-Mn $_{(E)}$	-21.83	1.08	V_{N}-Mn $_{(S)}$	-20.16	2.76
V_{N}-Fe $_{(E)}$	-21.43	1.48	V_{N}-Fe $_{(S)}$	-20.33	2.58
V_{N}-Co $_{(E)}$	-21.72	1.20	V_{N}-Co $_{(S)}$	-	-

Table S9 Cohesion energy of metal quadruple cluster and binding energy of transition metal on BC_3N_2 surface, where$\triangle E_{M}$ and $\triangle E_{VN-M}$ are the

Metal-site	$E_{M@BC3N2}$(eV）	$E_{VN-M@BC3N2}$	**Cohesive (eV)**		
			cluster of 4 atoms	$\triangle E_{M}$	$\triangle E_{VN-M}$
V-T_N	-2.65	-2.59	-2.15	-0.5	-0.44
Cr- T_N	-1.363	-1.071	-1.06	-0.303	-0.011
Mn- T_N	-1.275	-1.158	-1.13	-0.145	-0.028
Fe- T_N	-1.892	-2.265	-2.17	0.278	-0.095
Co- T_N	-2.549	-2.596	-2.25	-0.299	-0.346

References

S1 L. Fu, R. Wang, C. Zhao, J. Huo, C. He, K-H. Kim, W. Zhang, Construction of Cr-embedded graphyne electrocatalyst for highly selective reduction of CO_2 to CH_4: A DFT study, Chem. Eng. J. 414 (2021) 128857.